Supplemental data

Supplemental Results

Grouping of varieties based on specific classes of molecules

We characterized the three groups of varieties in more detail by building PCA models based on profiles of specific classes of molecules and by constructing an O2PLS-DA correlation plot. The PCA score scatter plots revealed the clear clustering of samples into three groups, as shown for the total metabolite content (**Figure 2A**), only for anthocyanins (**Supplementary Figure S10A**) and for flavonols and other flavonoids (**Supplementary Figure S10B**). In contrast, the analysis of hydroxybenzoic and hydroxycinnamic acids with hydroxytyrosol clearly separated Corvina from Sangiovese, and instead clustered with Merlot, Syrah and Cabernet Sauvignon (**Supplementary Figure S10C**). PCA plots of flavan-3-ols/proanthocyanins and stilbenes revealed sample scattering so that the six varieties could not be differentiated according to these molecules (data not shown). The correlation loading plot of O2PLS based on anthocyanins confirmed that class 1 (Merlot, Syrah and Cabernet Sauvignon) is characterized by malvidin, petunidin and delphinidin (acetyl) and (coumaroyl) 3-O-glucosides, class 3 (Oseleta) by cyanidin, peonidin and petunidin-3-O-glucoside, and Corvina and Sangiovese were negatively characterized by delphinidin-3-O-glucosides (**Supplementary Figure S10D** and **Supplementary Dataset S13)**. In the case of flavonols and other flavonoids, class 1 was characterized by a high content of acylated flavanones in particular the acetylated dihydrosyringetin, Oseleta by tetrahydroxy-monomethoxyflavanone, and Corvina and Sangiovese by dihydroquercetin (Taxifolin), kaempferol and quercetin-O-glucosides (**Supplementary Figure S10E and Supplementary Dataset S13).** Finally, the model for hydroxycinnamic and hydroxybenzoic acids revealed that Oseleta was characterized by a high content of hydroxycinnamic acids, Corvina by high levels of hydroxytyrosol, and that Merlot, Syrah, Cabernet Sauvignon and Sangiovese were characterized by an intermediate behavior between classes 2 and 3 (**Supplementary Figure S10F** and **Supplementary Dataset S13).**

More detailed metabolic characterization of intra-group varieties

Differences among the three varieties in group 1, and between the two in group 2, were characterized in more detail by building new PCA and O2PLS models (**Figure 2A**). Merlot, Syrah and Cabernet Sauvignon (group 1) were clearly separated by PCA (**Supplementary Figure S11A)** and the correlation loading plot of the resulting O2PLS model (R2X(cum): 0.735 and Q2(cum): 0.97) showed that Merlot was characterized by high stilbene and proanthocyanidin levels, Syrah

was distinguished by high levels of anthocyanin (coumaroyl)-3-O-glucosides, and Cabernet Sauvignon contained high levels of anthocyanin (acetyl)-3-O-glucosides (**Supplementary Figure S11B; Supplementary Dataset S14**). Corvina and Sangiovese (group 2) (**Figure 2A**) were distinguished by the high content of hydroxytyrosol and some flavonoids in Corvina and the high levels of some anthocyanin-3-O-glucosides in Sangiovese (**Supplementary Figure S11C and D**; **Supplementary Dataset S15).**

Supplemental Figures

Figure S1.

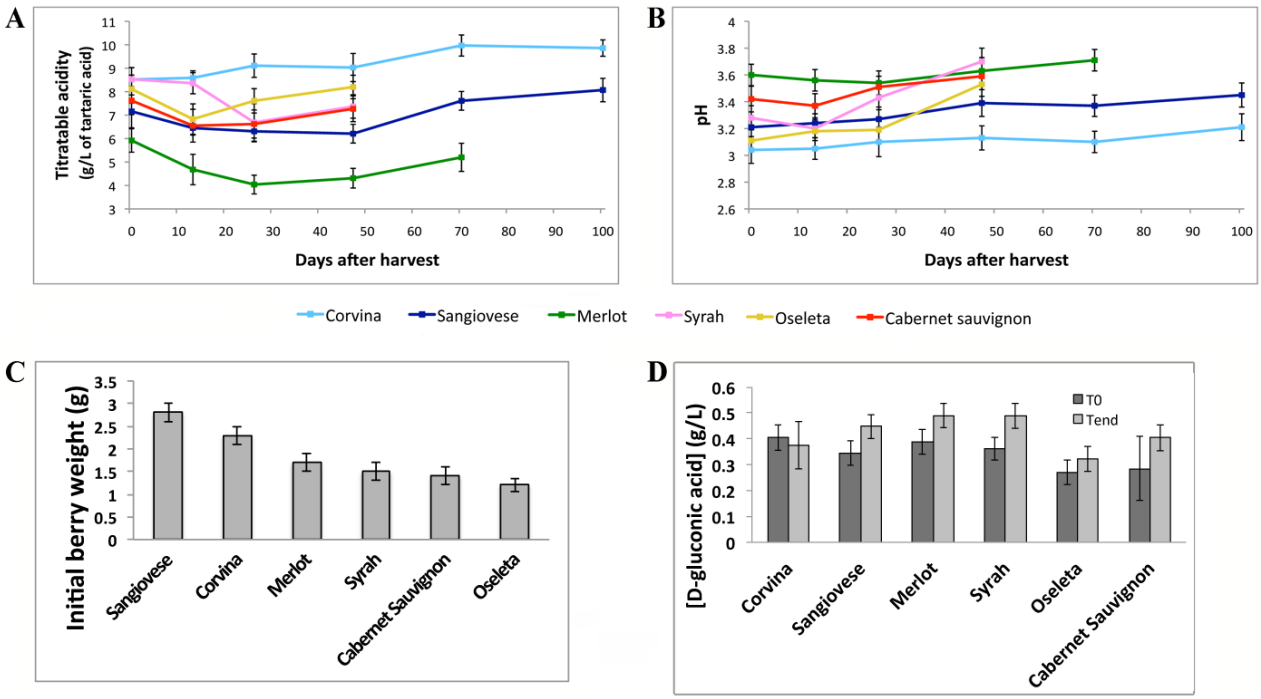

Figure S1. Overview of the postharvest dehydration process. **A** and **B,** Titratable acidity and pH trends. **C**, Initial berry weight of the six varieties. **D**, D-gluconic acid content at the T0 and Tend in the six genotypes.

Figure S2.

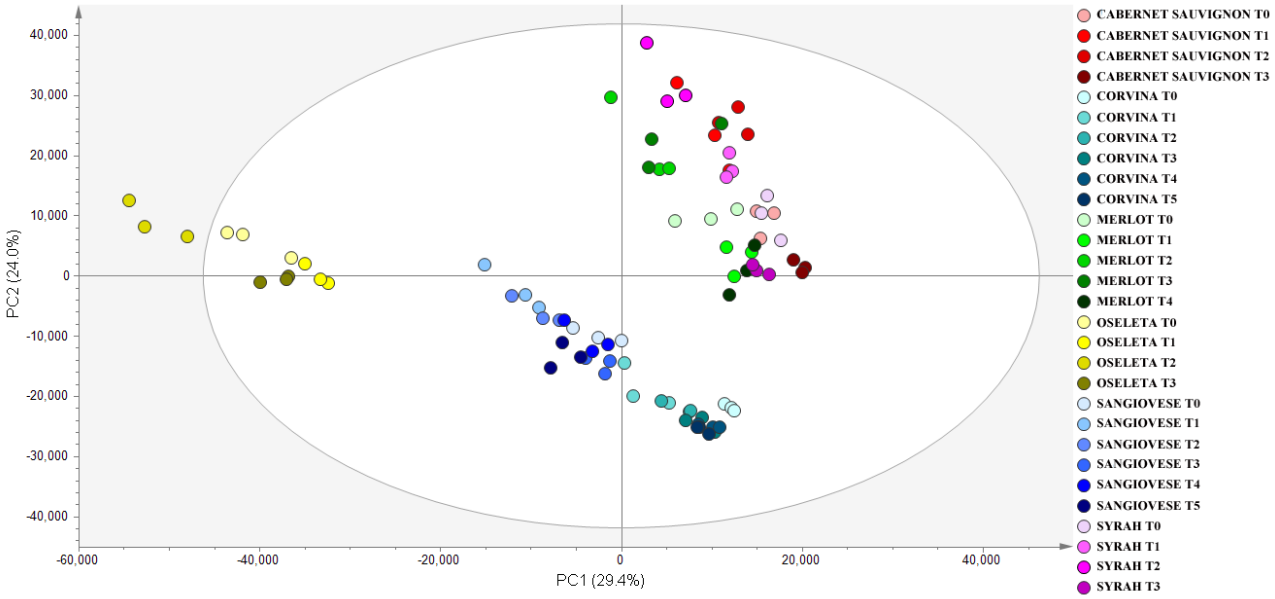

Figure S2. PCA score scatter plot of the model obtained for the metabolites detected by HPLC-ESI-MS in the six genotypes in all stages of postharvest. PCA score scatter plot is colored according to variety.

Figure S3.

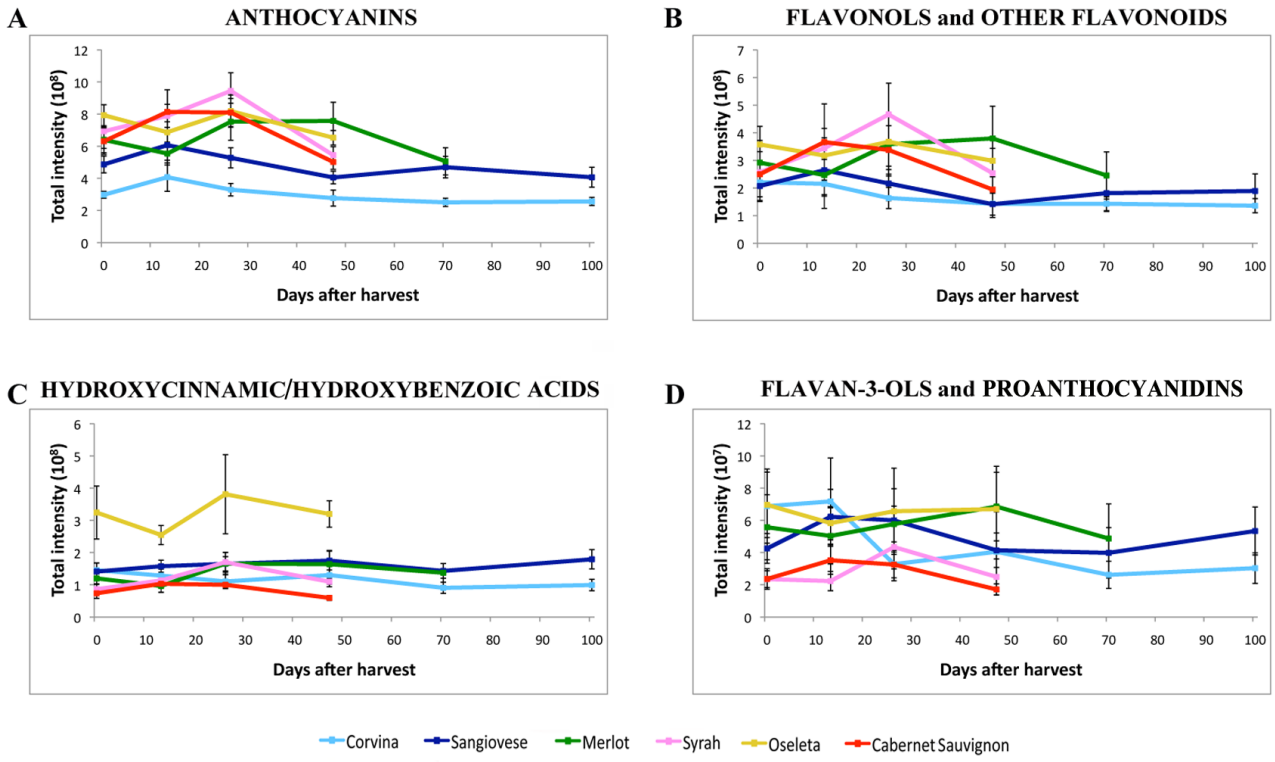

Figure S3. Accumulation trends of anthocyanins (**A**), flavonols and other flavonoids (**B**), hydroxycinnamic/hydroxybenzoic acids (**C**) and flavan-3-ols and proanthocyanindins (**D**) during the postharvest process in the six varieties. Values were determined by HPLC-MS analysis and indicated as sum of the peak areas (arbitrary units).

Figure S4.

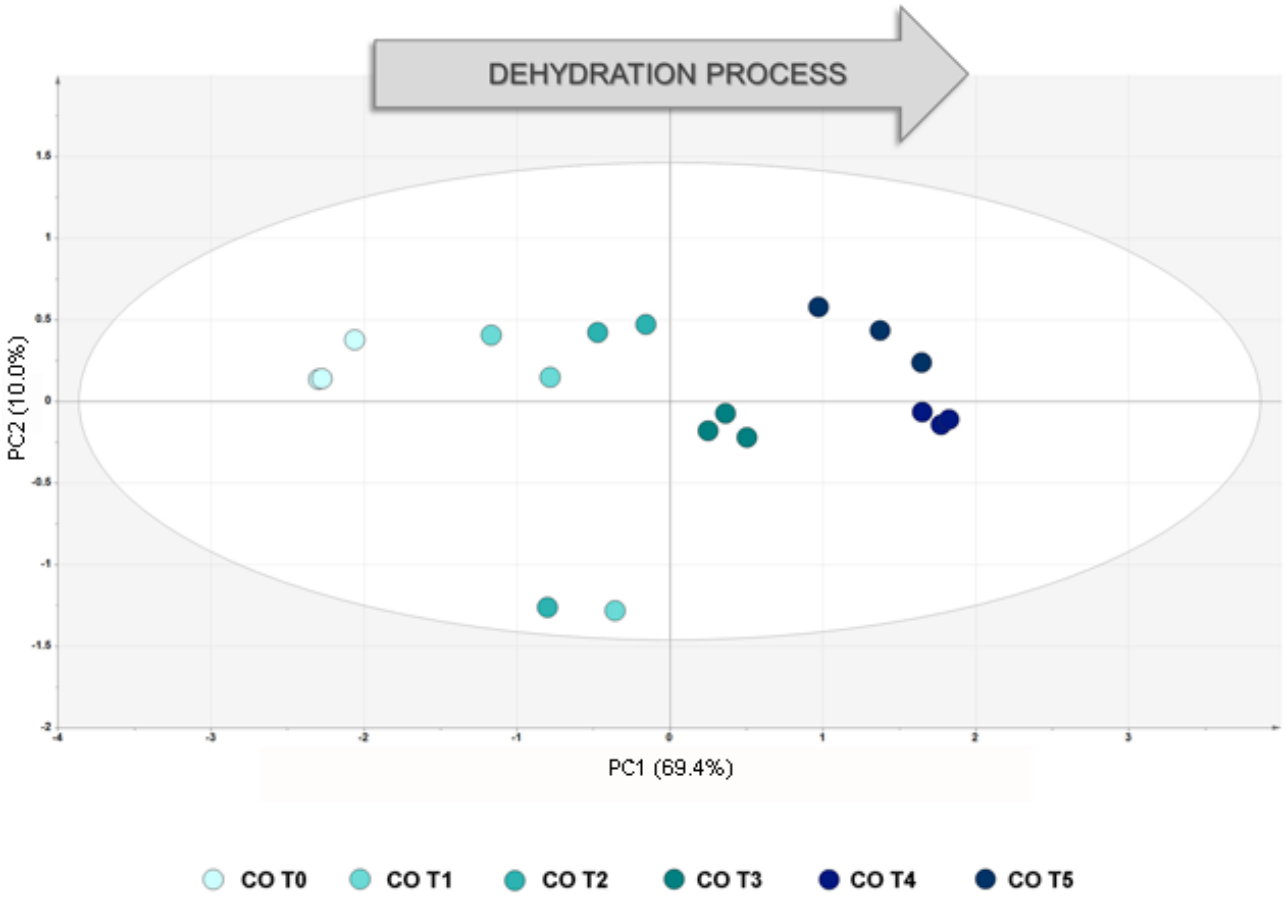

Figure S4. PCA score scatter plot of the model obtained for the volatile metabolites detected by GC-MS in all stages of Corvina berries. PCA score scatter plot is colored according to postharvest stage.

Figure S5.

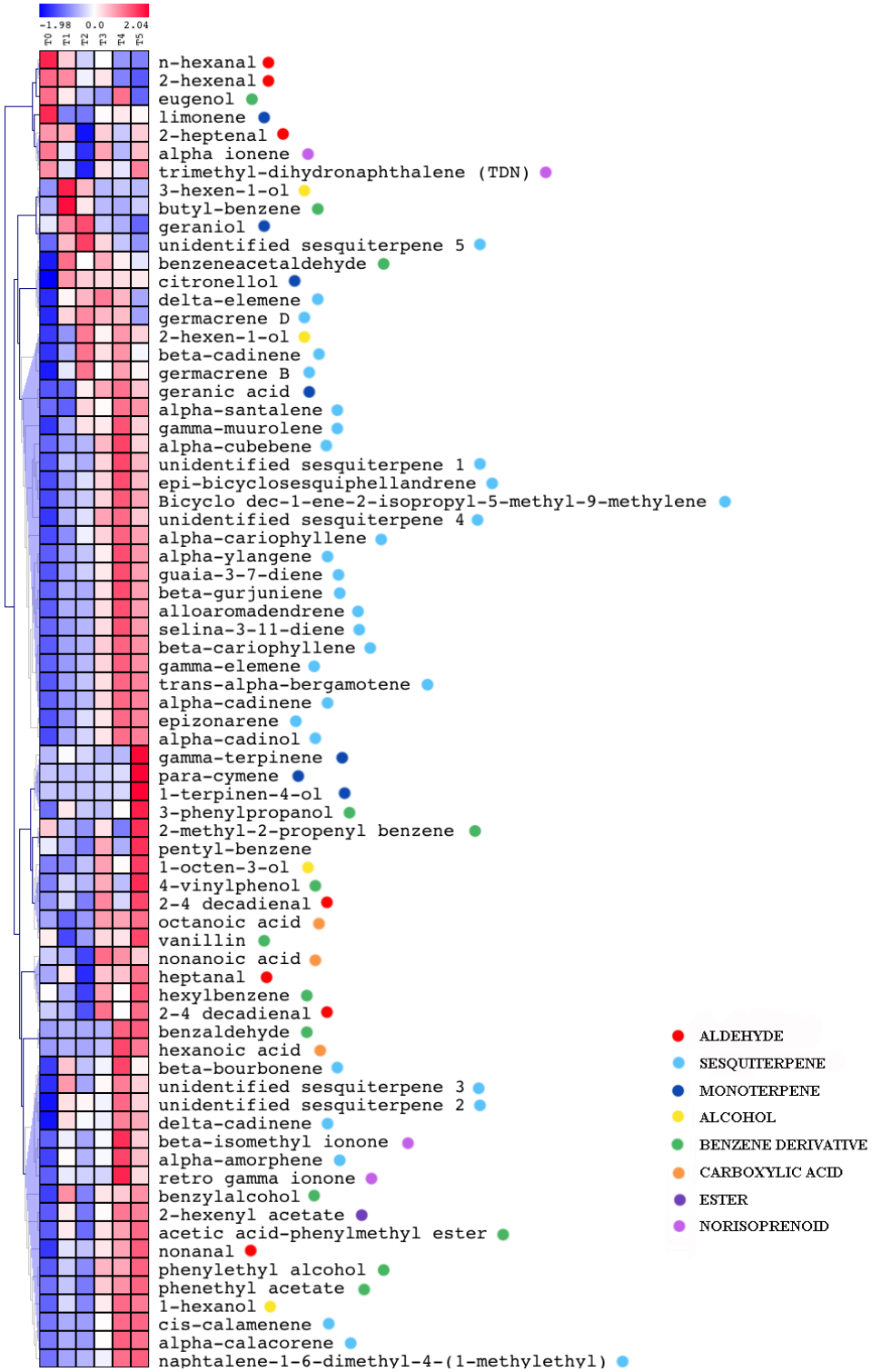

Figure S5. Hierarchical clustering of volatile organic compounds modulation during postharvest in Corvina berries. The heat map describes the accumulation (red) or depletion (blue) of each detected metobolite. The 72 compounds were included in eight classes of molecules described by different colors. Data have been normalized for berry weight loss and row mean centered (TmeV 4.4).

Figure S6.

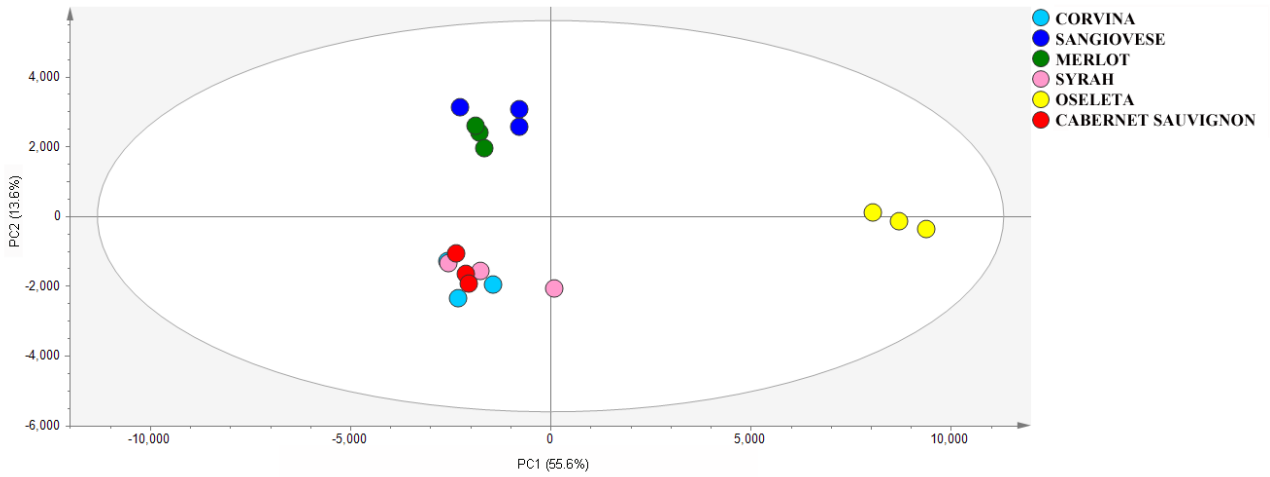

Figure S6. PCA score scatter plot of the model obtained for the transcripts detected by microarray analysis at harvest in each variety (explained variance = 69.2%). PCA score scatter plot is colored according to variety.

Figure S7.

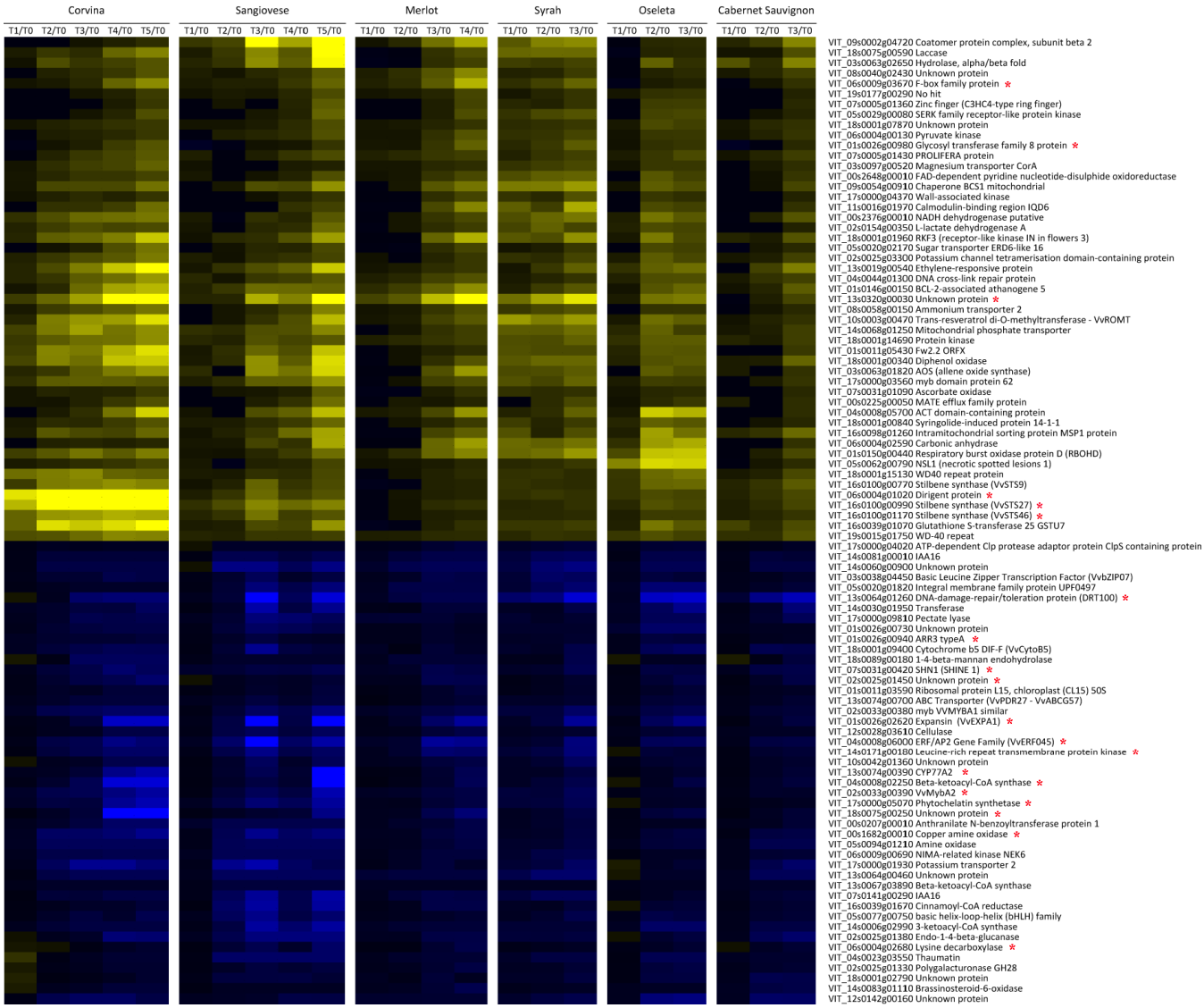

Figure S7. Heat map of commonly differentially modulated genes in the six genotypes during the postharvest process. Asterisk indicates genes also associated to the final and initial stages of the process identified by PCA.

Figure S8.

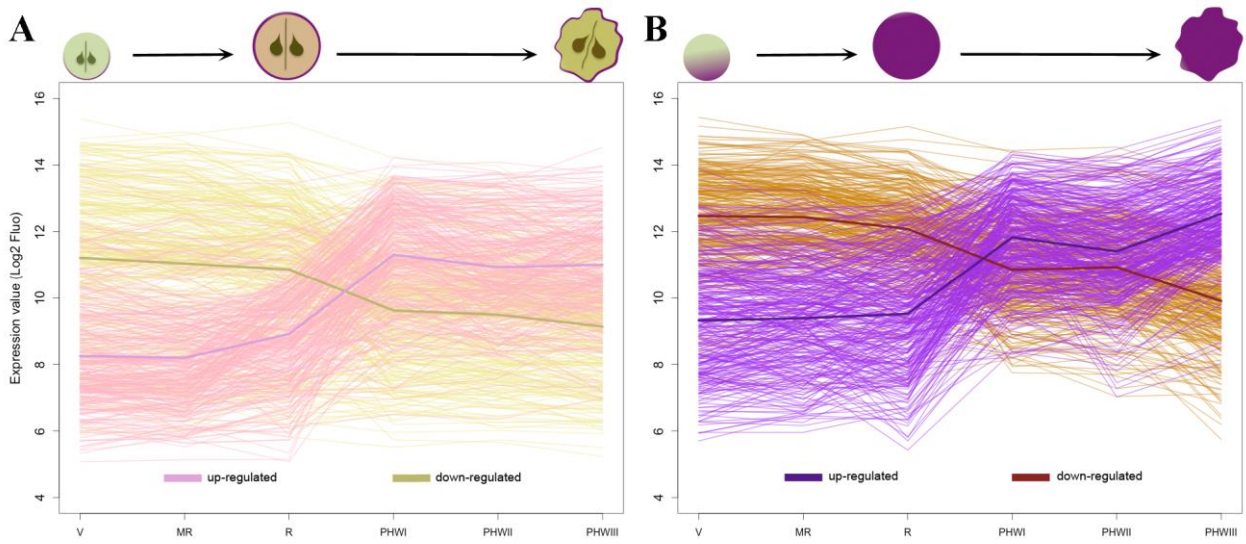

Figure S8. Gene expression of the most up-regulated (1st percentile) and down-regulated (99th percentile) Corvina transcripts we identified during the ripening and postharvest process in Corvina pulp (**A**) and skin (**B**), as reported in the expression atlas (Fasoli et al., 2012).

Figure S9.

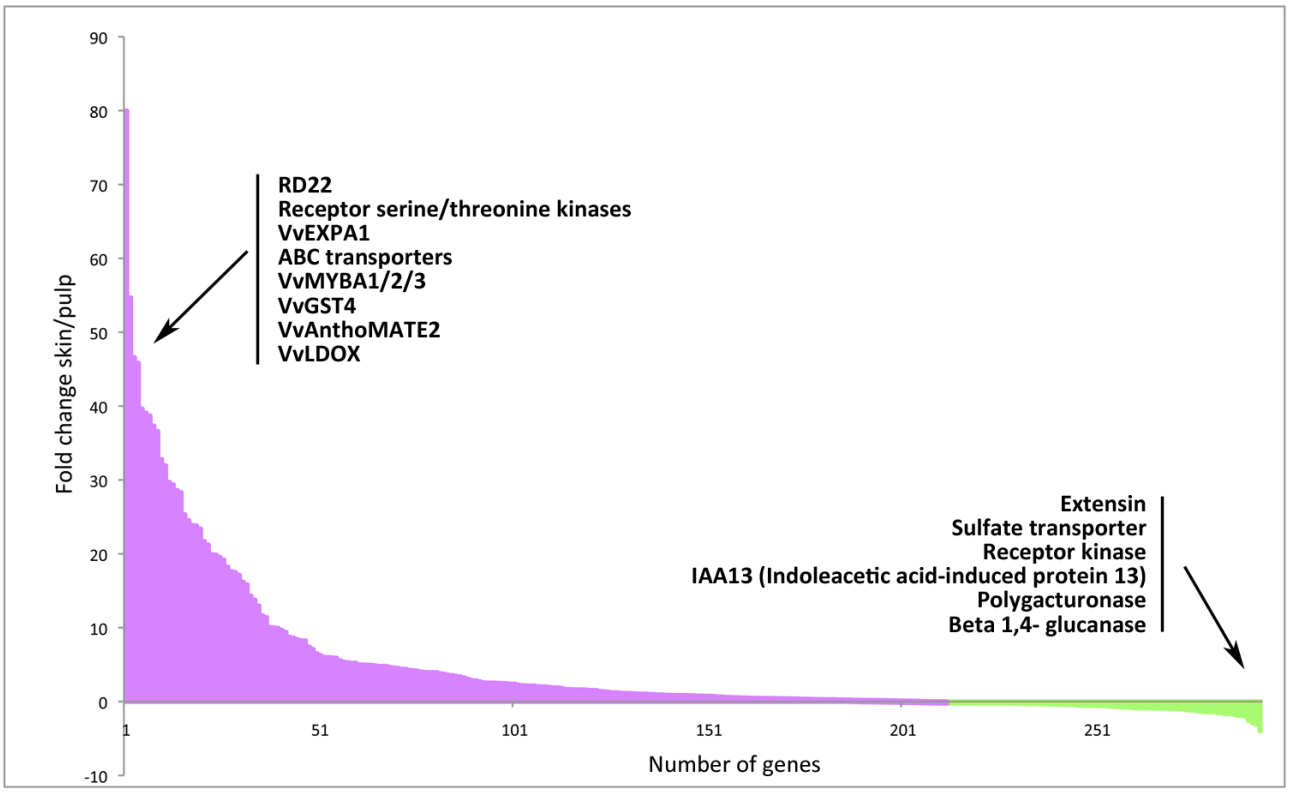

Figure S9. Ratio of the average expression level in the three postharvest stages analyzed by Fasoli et al., (2012) in pulp and skin of most downregulated genes. Positive fold changes are shown in pink and negative fold changes are shown in green.

Figure S10.

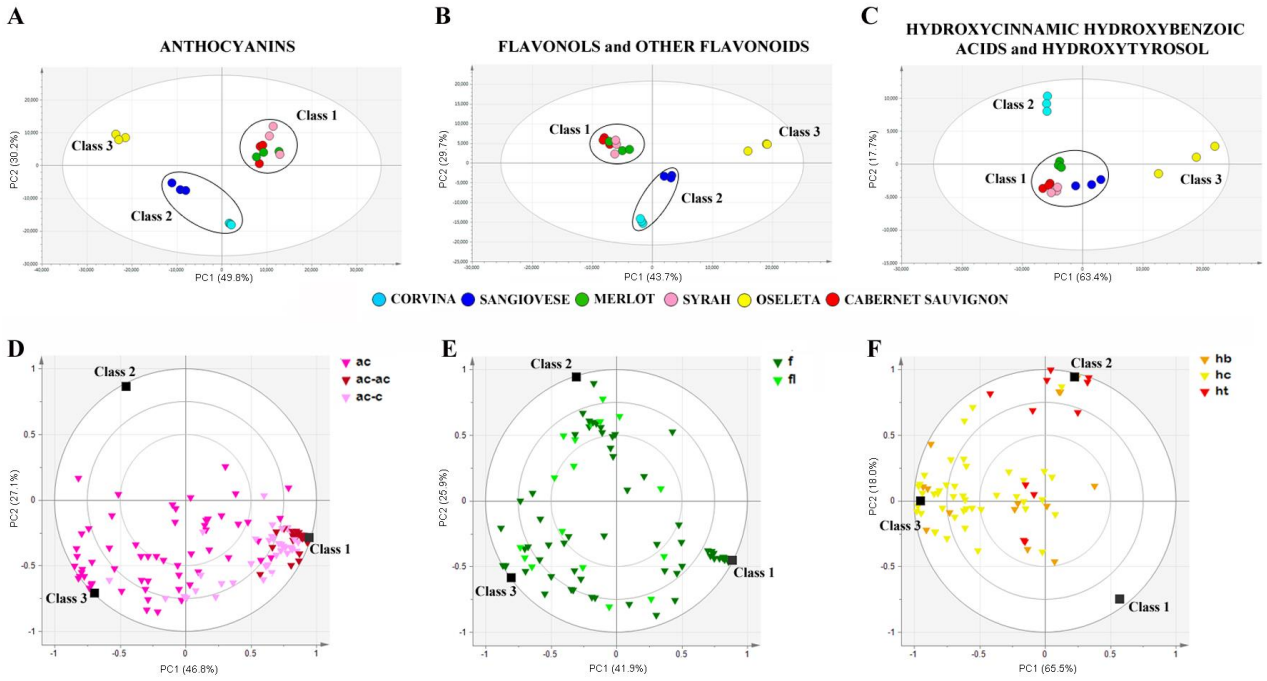

Figure S10. PCA score scatter plots of the models obtained for anthocyanins **(A),** flavonols and other flavonoids **(B),** and hydroxycinnamic, hydroxybenzoic acids and hydroxytyrosol **(C),** detected by HPLC-ESI-MS at harvest in the six varieties. O2PLS-DA correlation loading plots of the three-class models for the anthocyanins (**D**), flavonols and other flavonoids **(E),** and hydroxycinnamic, hydroxybenzoic acids and hydroxytyrosol **(F),** according to the unsupervised PCAs. Groups of metabolites are shown in different colors. Abbreviations: ac = anthocyanins; ac-ac = acylated anthocyanins; ac-c = coumaroyl anthocyanins; f = other flavonoids; fl = flavonols; hb = hydroxybenzoic acids; hc = hydroxycinnamic acids; ht = hydroxytyrosol.

Figure S11.

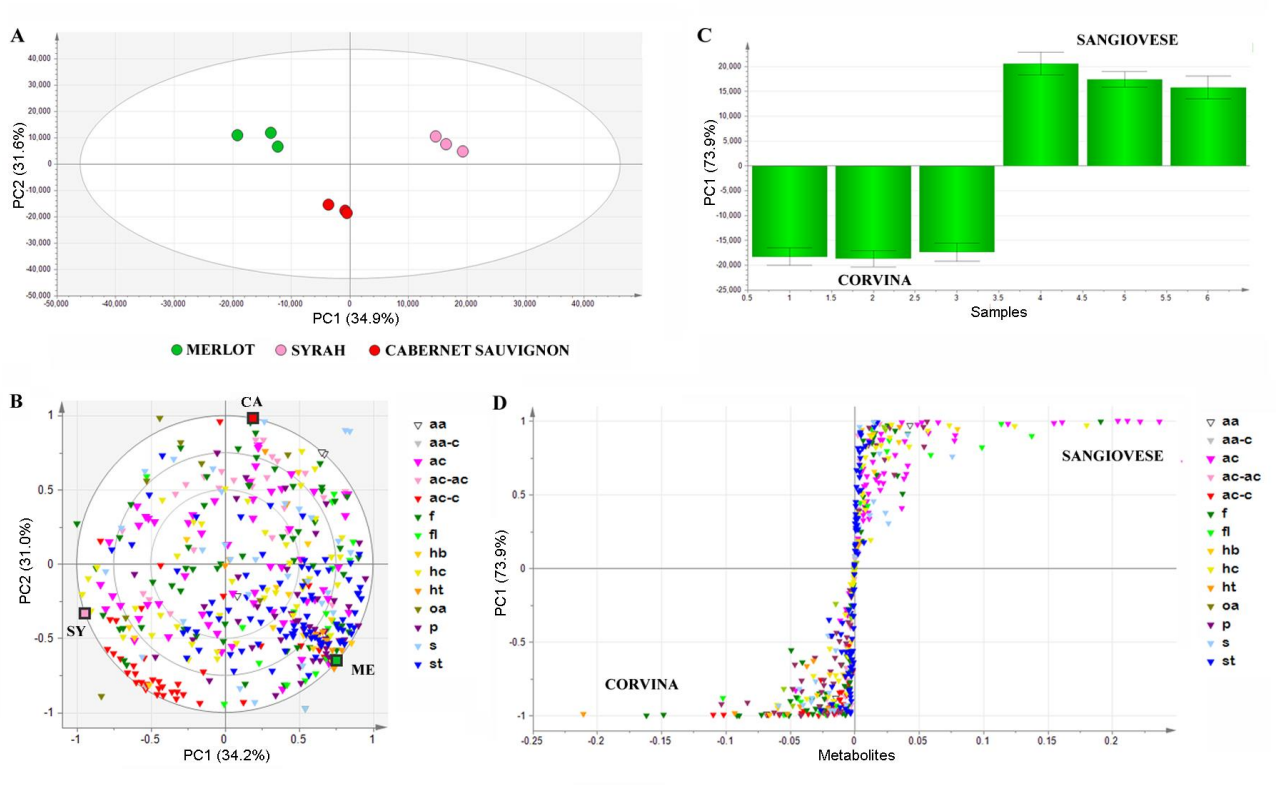

Figure S11. A, PCA score scatter plot of the model obtained for the metabolites detected by HPLC-ESI-MS at harvest for Merlot, Cabernet Sauvignon and Syrah, **B**, O2PLS-DA correlation loading plot of the three-class model according to the unsupervised PCA in **A. C,** PCA score column plot of the model obtained for the metabolites detected by HPLC-ESI-MS at harvest for Corvina and Sangiovese at harvest**, D,** O2PLS-DA correlation loading plot of the two-class model according to the unsupervised PCA in **C.** Groups of metabolites are shown in different colors. Abbreviations: CA= Cabernet Sauvignon; ME= Merlot; SY= Syrah; aa = amino acids; ac = anthocyanin; ac-ac = acylated anthocyanins; ac-c = coumaroyl anthocyanins; f = other flavonoids; fl = flavonols; hb = hydroxybenzoic acids; hc = hydroxycinnamic acids; ht = hydroxytyrosol; oa = organic acid; p = procyanidins; s = sugars; st = stilbenes.